

Extracting the time-domain building response from random vibrations*

Roel Snieder

Center for Wave Phenomena and Dept. of Geophysics,
Colorado School of Mines, Golden CO 80401
email rsnieder@mines.edu

Abstract

The extraction of the response from field fluctuations excited by random sources has received considerable attention in a variety of different fields. I show application of this principle to the motion recorded in the Millikan library at the California Institute of Technology in Pasadena, California, after an earthquake. Deconvolution of the recorded motion at different floors unravels the building response from the complicated excitation and from the unknown soil-structure interaction. I give arguments why analyzing the response function in the time domain is more informative than just using the amplitude spectrum of the transfer function. I provide examples that show that it is possible to extract the building response that satisfies the same dynamic equations as does the real building, but that may satisfy different boundary conditions at the base. This means one can obtain from the data the building response with different soil-structure interaction than the real building has.

1 Introduction

The extraction of information from random field fluctuations is a rapidly growing field in physics, acoustics, engineering, and geophysics. The widespread application of this idea has led to a variety of different names used for the method that include Green's function extraction, daylight imaging, the virtual source method, and seismic interferometry [1, 2].

Aki [3] pioneered the use of microseismic noise to extract the properties of the near surface; a technique that later was called microtremor analysis and that found numerous applications [4, 5]. Lobkis and Weaver [6] gave the field new momentum with their derivation of Green's function extraction based on normal modes, and they showed how useful the Green's function extraction can be in practical applications. A flurry of applications appeared in different fields that include ultrasound [7, ?, 8, 9, 10], helioseismology [11, 12], ocean acoustics [13, 14, 15], structural engineering [16, 17, 18, 19, 20], medical diagnostics [21], exploration seismology [22, 23, 24, 25, 26], crustal seismology [27, 28, 29, 30, 31, 32], and hazard monitoring [33, 34, 35]. In most of the applications the system response was extracted by cross-correlating field fluctuations, but the alternative data-processing technique of deconvolution has been applied in some of these studies.

The fields obtained from correlation or deconvolution satisfy the same equation as does the original system; these methods are thus guaranteed to give valid states of the field in the real

*This chapter is published as: Snieder, R., Extracting the time-domain building response from random vibrations, in Coupled site and soil-structure interaction effects with application to seismic risk mitigation, eds. T. Schanz and R. Iankov, p.283-292, Springer, 2009

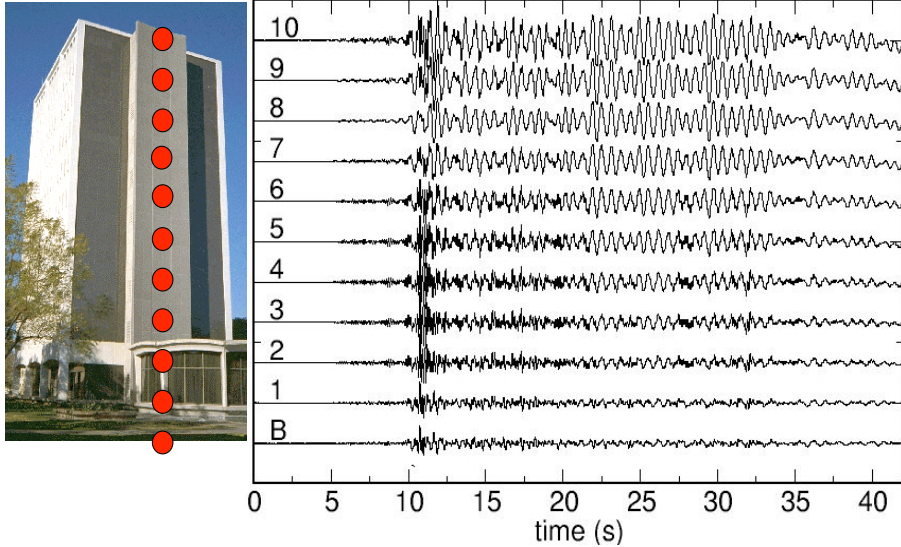


Figure 1: Left panel: the Millikan library at Caltech with the location of accelerometers. Right panel: north-south component of acceleration after the Yorba Linda earthquake of 03 Sep 2002 (ML=4.8, Time: 02:08:51 PDT, 33.917N 117.776W Depth 3.9km). Traces are labeled with the floor number (B indicates basement).

medium [17]. The field extracted with any of the three approaches may, however, satisfy different boundary conditions than the real physical system satisfies. This makes it possible to determine the wave state as if the system satisfied different boundary conditions than the real system does.

I illustrate the extraction of the system response by showing in section 2 the response extracted from a building from the recorded motion of the building after an earthquake. In section 3 I show advantages of extracting the transfer function in the time domain, rather than considering only the amplitude spectrum of the impulse response. Section 4 contains examples of the extracted wave state of the building as if it was placed on the reflection-less subsurface, or on a subsurface that gives total reflection.

2 Extracting the building response

I illustrate the extracting the time-domain response of a building from random vibrations with recordings of the motion of the Millikan library at Caltech extracted from recorded vibrations of the building after an earthquake [16]. This building is shown in the left panel of figure 1 and the location of accelerometers in the basement and the 10 floors is marked with solid circles. The north-south component of the acceleration after the Yorba Linda earthquake is shown in the right panel. The motion increases with height in the building because of the increased sway of the building with height.

The recorded motion is a consequence of the combination of (i) the waves excited by the earthquake that strike the building from below, (ii) the coupling of the building to the subsurface, and (iii) the mechanical properties of the building. It is the goal to extract the mechanical properties of the building from the motion shown in figure 1. This can be achieved by deconvolving the motion at every level with the motion recorded at one of the floors. Deconvolution of the motion $u(z, t)$ at

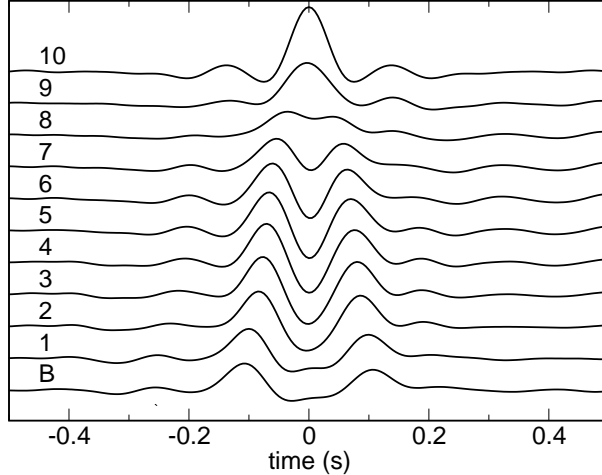


Figure 2: Waveforms of figure 1 after deconvolution with the motion at the top floor.

height z , with the motion $u(z_0, t)$ at reference level z_0 , is, in the frequency domain, given by:

$$D(z, z_0, \omega) = \frac{u(z, \omega)}{u(z_0, \omega)}, \quad (1)$$

where $u(z, \omega)$ is the temporal Fourier transform of $u(z, t)$. At notches in the spectrum $u(z_0, \omega)$ this spectral division is unstable. For this reason I replace the deconvolution in expression (1) by

$$D(z, z_0, \omega) = \frac{u(z, \omega)u^*(z_0, \omega)}{|u(z_0, \omega)|^2 + \varepsilon}. \quad (2)$$

Figure 2 shows the motion of the Millikan library after deconvolution with the motion at the top floor. The deconvolved motion in the top of the building is a bandpass-filtered delta function in the basement, because any function deconvolved with itself gives a delta function. The deconvolved waves are extremely simple and consist of an upgoing wave that propagates up the building, is reflected by the top of the building, and then propagates downward. The velocity of this wave can easily be measured and is equal to 322 m/s [16]. During their propagation through the building, the deconvolved waves attenuate, and the quality factor of the building can be estimated from the attenuation [16].

The response extracted by deconvolving the motion at every floor with the motion in the basement is shown in figure 3. Now the motion in the basement is a bandpass-filtered delta function. Note that these deconvolved waveforms are more complicated than those in figure 2. The motion in figure 3 is for early time ($t < 1$ s) given by a superposition up upward and downward propagating waves. For later time the motion has a harmonic character and is dominated by the motion of the fundamental mode of the building.

Note that the motion in figure 3 is causal, while the motion in figure 2 is not. The Millikan library is excited at its base, and the response shown in figure 3 shows the response to this excitation. This response is causal because the motion of the building follows the excitation in time. In contrast, the deconvolved motion in figure 2 is nonzero for negative time. This is due to the absence of a source at the top of the building. By definition, the deconvolved motion of this wave state is a bandpass filtered delta function centered at $t = 0$ at the top of the building. The only way to generate this

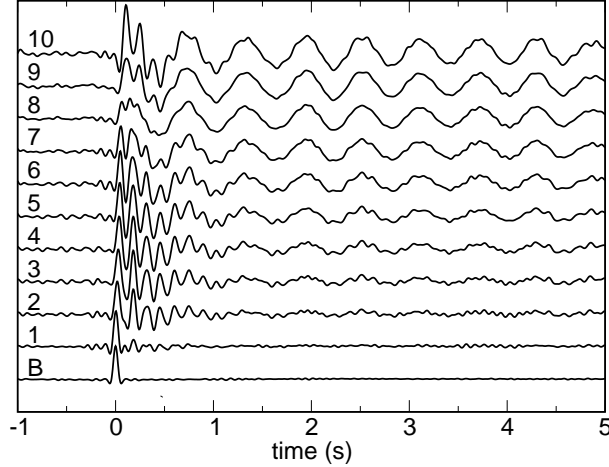


Figure 3: Waveforms of figure 1 after deconvolution with the motion in the basement. Note that the time scale is different than in figure 2.

impulsive motion at the top of the building in the absence of a source at that location is to send a wave upward in the building that arrives at the top at $t = 0$. In order to achieve this, the wave must be launched from the base of the building at negative time, and this is exactly what can be seen in figure 2.

3 Time domain versus frequency domain response

As an alternative to the deconvolved waveforms in the time domain one could analyze the amplitude spectrum of the motion recorded in figure 1. The amplitude spectrum thus obtained is the product of the amplitude spectra of the waves striking the building from below, the ground coupling, and the building response. In this approach the contribution of these three physical contribution are still mixed. In order to eliminate the contribution of the unknown excitation the amplitude of the spectral ratio of expression (1) in the frequency domain is often considered.

As an example, let us consider what this amplitude ratio gives for the deconvolved waves shown in figure 2. At any level, the deconvolved motion is approximately given by

$$D(t) = s(t + \tau) + s(t - \tau), \quad (3)$$

where $\pm\tau$ are the arrival times of the upgoing and downgoing waves, respectively. For simplicity I ignore attenuation and assume that the amplitudes of the upgoing and downgoing waves are identical. In the frequency domain this expression corresponds to

$$D(\omega) = (e^{-i\omega\tau} + e^{i\omega\tau}) s(\omega) = 2 \cos(\omega\tau) S(\omega), \quad (4)$$

with $S(\omega)$ the Fourier transform of the band-limited delta function $s(t)$. The amplitude of this spectral ration is given by

$$|D(\omega)| = 2 |\cos(\omega\tau)| |S(\omega)|, \quad (5)$$

while the phase φ satisfies

$$\tan(\varphi) = \frac{\text{Im}(S(\omega))}{\text{Re}(S(\omega))}. \quad (6)$$

The time domain deconvolved waves of expression (3) are trivial to interpret; they consist of two waves arriving at opposite arrival times. In contrast, if one only knew the amplitude spectrum (4) it would not be trivial to infer that the deconvolved motion consist of just two waves with opposite arrival time because the information of the arrival time, $|\cos(\omega\tau)|$, is multiplied with the amplitude spectrum $|S(\omega)|$ of the band-limited delta function. Information of the travel time τ is encoded in the notches of the deconvolved spectra, which may be difficult to interpret.

Note that the phase φ in expression (6) does not depend on the travel time τ at all, hence the phase is useless to infer that that waves consist of upgoing and downgoing waves with opposite travel time τ . If one arbitrarily changes the origin of the time axis in figure 2 over a time shift t_0 , the phase is given by

$$\tan(\varphi) = \frac{\text{Im}(S(\omega))}{\text{Re}(S(\omega))} - \omega t_0 . \quad (7)$$

The measured phase is restricted to lie between 0 and 2π , and after the phase wrapping the measured phase is a complicated function of frequency, that carries no information about the travel time τ at all.

This analysis of the waves in figure 2 illustrates the advantages of analyzing the deconvolved response in the time-domain rather than in the frequency domain. When the motion in a system consists of the superposition of a limited number of resonances it is, of course, informative to study the amplitude spectrum of the deconvolved motion because this provides direct information of the frequency of these resonances. In the example of the motion deconvolved with the motion in the basement (figure 3) this procedure gives the frequency of the normal mode of the building. There is, of course, no reason why one could not analyze both the time dependence and the amplitude spectrum of the deconvolved response. This can be useful because these different quantities provide complementary information of the building response.

4 Changing the boundary conditions

It is not widely known that in the Green's function extraction one can alter the boundary conditions of the system. For the correlation and deconvolution approaches the extracted response satisfies the same field equation as does the physical system [17].

I illustrate the freedom to change the boundary conditions in seismic interferometry with the response of the Millikan library at Caltech extracted from recorded vibrations of the building after an earthquake shown in figure 1. Figure 2 shows the motion of the Millikan library after deconvolution with the motion at the top floor. The motion at the top floor is collapsed into a bandpass-filtered delta function because the recorded motion at the top floor is deconvolved with itself, and the deconvolution of any function with itself yields a delta function. The response in figure 2 is a-causal, but it still is a valid wave state of the building that consists of one upgoing wave that is reflected by the top of the building into a downgoing wave. Note that this downgoing wave is not reflected at the base base of the building, this wave state thus corresponds to a fictitious building that has reflection coefficient $R = 0$ at its base. This example shows that response extracted by this deconvolution makes it possible to determine the building response for the hypothetical situation that the building would have been placed on a reflection-free subsurface.

The response extracted by deconvolving the motion at every floor with the motion in the basement is shown in figure 3. The extracted response in the basement is a bandpass-filtered delta function because it consists of the motion in the basement deconvolved with itself. Since the delta function is equal to zero for $t \neq 0$, the extracted motion in the basement vanishes for non-zero time. In the real building, the motion at the base does, of course, not vanish for $t \neq 0$. In fact,

one can see in the bottom trace of the original data in figure 1 that the building is being shaken at its base throughout the arrival of the body wave coda and the surface waves that excite the building. In contrast, the extracted response in figure 3 is for a fictitious building whose base is excited by a bandpass filtered delta pulse and then remains fixed. Such a fictitious building has reflection coefficient $R = -1$ at the base [17], which precludes the transmission of energy from the subsurface into the building!

The examples of figures 2 and 3 show that from one data set one can retrieve wave-states that satisfy different boundary conditions. The real building has neither reflection coefficient $R = 0$ nor $R = -1$ at its base. A reflection coefficient $R = 0$ precludes the resonance that is clearly visible in figure 1 because for a reflection-less ground coupling all wave energy is radiated downward at the base. If the reflection coefficient at the base of the real building would be given by $R = -1$, energy would not be able to be transmitted into the building. Additional examples of wave-states of the building that have reflection coefficient $R = 0$, but that are either purely causal or a-causal can be found in ref. [17]. Note that the extracted response in the figures 2 and 3 is solely based on data-processing of the recorded motion in figure 1.

5 Conclusion

The example of the motion of the Millikan library shows that deconvolution is an effective method to extract the building response from recorded motion after a complicated excitation by an earthquake. The retrieved time-domain response shows distinct waves arriving. One can measure the velocity and attenuation of these waves and retrieve the velocity of shear waves and the associated attenuation of the building. Extracting such information from the amplitude spectrum of the impulse response is much more difficult because arrival time information is coded in a complicated way into the notches of the extracted spectral amplitude. The examples shown in this work show that it is possible to extract the time-domain response of structures under different boundary conditions than does the real structure. This can be a valuable tool for obtaining independent estimates of the building response from the soil-structure interaction. Note that the extraction of the building response under different boundary conditions at the base does only involve data-processing; it does not entail numerical modeling of the building, and the mechanical properties of the building need not be known. We have applied interferometric techniques that change the boundary conditions in marine exploration seismology with the goal of suppressing waves that are reflected from the ocean's free surface [36, 37].

Acknowledgments: this work was supported by the NSF (grant EAS-0609595), and by the GameChanger program of Shell.

References

- [1] A. Curtis, P. Gerstoft, H. Sato, R. Snieder, and K. Wapenaar. Seismic interferometry – turning noise into signal. *The Leading Edge*, 25:1082–1092, 2006.
- [2] E. Larose, L. Margerin, A. Derode, B. van Tiggelen, M. Campillo, N. Shapiro, A. Paul, L. Stehly, and M. Tanter. Correlation of random wavefields: an interdisciplinary review. *Geophysics*, 71:SI11–SI21, 2006.
- [3] K. Aki. Space and time spectra of stationary stochastic waves with special reference to microtremors. *Bull. of the Earthquake Res. Inst.*, 35:415–456, 1957.

- [4] J.N. Louie. Faster, better: Shear-wave velocity to 100 meters depth from refraction microtremor analysis. *Bull. Seismol. Soc. Am.*, 91:347–364, 2001.
- [5] F.J. Chávez-Garcia and F. Luzón. On the correlation of seismic microtremors. *J. Geophys. Res.*, 110:B11313, doi:10.1029/2005JB003686, 2005.
- [6] O.I. Lobkis and R.L. Weaver. On the emergence of the Green’s function in the correlations of a diffuse field. *J. Acoust. Soc. Am.*, 110:3011–3017, 2001.
- [7] R.L. Weaver and O.I. Lobkis. Ultrasonics without a source: Thermal fluctuation correlations at MHz frequencies. *Phys. Rev. Lett.*, 87:134301, 2001.
- [8] A. Malcolm, J. Scales, and B.A. van Tiggelen. Extracting the Green’s function from diffuse, equipartitioned waves. *Phys. Rev. E*, 70:015601, 2004.
- [9] K. van Wijk. On estimating the impulse response between receivers in a controlled ultrasonic experiment. *Geophysics*, 71:SI79–SI84, 2006.
- [10] E. Larose, G. Montaldo, A. Derode, and M. Campillo. Passive imaging of localized reflectors and interfaces in open media. *Appl. Phys. Lett.*, 88:104103, 2006.
- [11] J.E. Rickett and J.F. Claerbout. Acoustic daylight imaging via spectral factorization; helioseismology and reservoir monitoring. *The Leading Edge*, 18:957–960, 1999.
- [12] J.E. Rickett and J.F. Claerbout. Calculation of the sun’s acoustic impulse response by multi-dimensional spectral factorization. *Solar Physics*, 192:203–210, 2000.
- [13] P. Roux and M. Fink. Green’s function estimation using secondary sources in a shallow water environment. *J. Acoust. Soc. Am.*, 113:1406–1416, 2003.
- [14] P. Roux, W.A. Kuperman, and NPAL Group. Extracting coherent wave fronts from acoustic ambient noise in the ocean. *J. Acoust. Soc. Am.*, 116:1995–2003, 2004.
- [15] K.G. Sabra, P. Roux, A.M. Thode, G.L. D’Spain, and W.S. Hodgkiss. Using ocean ambient noise for array self-localization and self-synchronization. *IEEE J. of Oceanic Eng.*, 30:338–347, 2005.
- [16] R. Snieder and E. Şafak. Extracting the building response using seismic interferometry; theory and application to the Millikan library in Pasadena, California. *Bull. Seismol. Soc. Am.*, 96:586–598, 2006.
- [17] R. Snieder, J. Sheiman, and R. Calvert. Equivalence of the virtual source method and wavefield deconvolution in seismic interferometry. *Phys. Rev. E*, 73:066620, 2006.
- [18] D. Thompson and R. Snieder. Seismic anisotropy of a building. *The Leading Edge*, 25:1093, 2006.
- [19] M.D. Kohler, T.H. Heaton, and S.C. Bradford. Propagating waves in the steel, moment-frame Factor building recorded during earthquakes. *Bull. Seismol. Soc Am.*, 97:1334–1345, 2007.
- [20] K.G. Sabra, A. Srivastava, F.L. di Scalea, I. Bartoli, P. Rizzo, and S. Conti. Structural health monitoring by extraction of coherent guided waves from diffuse fields. *J. Acoust. Soc. Am.*, 123:EL8–EL13, 2008.

- [21] K.G. Sabra, S. Conti, P. Roux, and W.A. Kuperman. Passive in-vivo elastography from skeletal muscle noise. *Appl. Phys. Lett.*, 90:194101, 2007.
- [22] G.T. Schuster, J. Yu, J. Sheng, and J. Rickett. Interferometric/daylight seismic imaging. *Geophys. J. Int.*, 157:838–852, 2004.
- [23] A. Bakulin and R. Calvert. The virtual source method: Theory and case study. *Geophysics*, 71:SI139–SI150, 2006.
- [24] B.E. Hornby and J. Yu. Interferometric imaging of a salt flank using walkaway VSP data. *The Leading Edge*, 26:760–763, 2007.
- [25] D. Draganov, K. Wapenaar, W. Mulder, J. Singer, and A. Verdel. Retrieval of reflections from seismic background-noise measurements. *Geophys. Res. Lett.*, 34:L04305, 2007.
- [26] A. Bakulin, A. Mateeva, K. Mehta, P. Jorgensen, J. Ferrandis, I. Sinha Herhold, and J. Lopez. Virtual source applications to imaging and reservoir monitoring. *The Leading Edge*, 26:732–740, 2007.
- [27] M. Campillo and A. Paul. Long-range correlations in the diffuse seismic coda. *Science*, 299:547–549, 2003.
- [28] N.M. Shapiro and M. Campillo. Emergence of broadband Rayleigh waves from correlations of the ambient seismic noise. *Geophys. Res. Lett.*, 31:L07614, doi:10.1029/2004GL019491, 2004.
- [29] N.M. Shapiro, M. Campillo, L. Stehly, and M.H. Ritzwoller. High-resolution surface-wave tomography from ambient seismic noise. *Science*, 307:1615–1618, 2005.
- [30] K.G. Sabra, P. Gerstoft, P. Roux, W.A. Kuperman, and M.C. Fehler. Surface wave tomography from microseisms in Southern California. *Geophys. Res. Lett.*, 32:L14311, doi:10.1029/2005GL023155, 2005.
- [31] P. Roux, K.G. Sabra, P. Gerstoft, and W.A. Kuperman. P-waves from cross correlation of seismic noise. *Geophys. Res. Lett.*, 32:L19303, doi: 10.1029/2005GL023803, 2005.
- [32] K. Mehta, R. Snieder, and V. Graizer. Downhole receiver function: a case study. *Bull. Seismol. Soc. Am.*, 97:1396–1403, 2007.
- [33] K.G. Sabra, P. Roux, P. Gerstoft, W.A. Kuperman, and M.C. Fehler. Extracting coherent coda arrivals from cross-correlations of long period seismic waves during the Mount St. Helens 2004 eruption. *J. Geophys. Res.*, 33:L06313, doi:10.1029/2005GL025563, 2006.
- [34] C. Sens-Schönfelder and U. Wegler. Passive image interferometry and seasonal variations at Merapi volcano, Indonesia. *Geophys. Res. Lett.*, 33:L21302, doi:10.1029/2006GL027797, 2006.
- [35] U. Wegler and C. Sens-Schönfelder. Fault zone monitoring with passive image interferometry. *Geophys. J. Int.*, 168:1029–1033, 2007.
- [36] K. Mehta, A. Bakulin, J. Sheiman, R. Calvert, and R. Snieder. Improving the virtual source method by wavefield separation. *Geophysics*, 72:V79–V86, 2007.
- [37] K. Mehta, J.L. Sheiman, R. Snieder, and R. Calvert. Strengthening the virtual-source method for time-lapse monitoring. *Geophysics*, 73:S73–S80, 2008.